Core Effect on the Performance of N/P Co-doped Carbon Encapsulating Noble-metal Phosphide Nanostructures for Hydrogen Evolution Reaction

Jie Yu,[†] Xinhao Wu,[†] Haijuan Zhang,[†] Meng Ni,[‡] Wei Zhou,[,†] and Zongping Shao[*,†,§]*

[†]Jiangsu National Synergetic Innovation Center for Advanced Materials (SICAM), State Key Laboratory of Materials-Oriented Chemical Engineering, College of Chemical Engineering, Nanjing Tech University, No. 5, Xin Mofan Road, Nanjing 210009, P.R. China

[‡]Building Energy Research Group, Department of Building and Real Estate, The Hong Kong Polytechnic University, Hung Hom, Kowloon, 999077, Hong Kong, China

[§]Department of Chemical Engineering, Curtin University, Perth, Western Australia 6845, Australia

ABSTRACT: The concept of core-shell nanostructured catalysts with a highly active yet insufficient stability in direct contact with electrolyte solution core and a chemically stable carbon shell has been proposed and turned out to be a new category of electrocatalysts for various electrochemical reactions. Such catalysts can take the mutual benefits of the core, i.e., high activity, and the shell, i.e., the high stability. However, the understanding about how the core affects the electrocatalytic performance of the shell is still not clear. In this study, we carried out a systematic study on hydrogen evolution reaction (HER) catalytic activities of different noble-metal phosphides-based core-shell nanostructured hybrids (noble-metal phosphides nanoparticles wrapped by ultrathin N, P-codoped graphitic carbon (NPGC) shells, MP_x@NPGC, MP_x=RhP_2, RuP_2, PtP_2, IrP_2 and Pd_5P_2) in both acidic and alkaline aqueous solutions for the first time. Among them, RhP_2@NPGC core-shell nanostructure exhibited the highest HER activity in 0.5 M H_2SO_4, while the RuP_2@NPGC composite was the best one in 1 M KOH. Taking microstructure into account, it is obvious that the catalytic behavior of the MP_x@NPGC category was largely attributed to the different noble-metal phosphide cores. The ECSA normalized activity further revealed the RhP_2@NPGC and RuP_2@NPGC hybrids are the most active HER catalysts in acidic and alkaline electrolytes, respectively, along with fastest charge transfer and surface reaction rates during the HER process. This study provides useful guidelines in the further development of high-performance core-shell structured electrocatalysts for HER, and other electrochemical reactions such as oxygen evolution reaction and oxygen reduction reaction.

KEYWORDS: noble-metal phosphide, carbon shell, core-shell nanostructure, hydrogen evolution reaction, systematic study

1. INTRODUCTION

To relieve the burden on environmental deterioration and energy crisis from the extensive use of non-renewable fossil fuels, hydrogen, characterized by emission-free and carbon-zero nature and superior mass-specific energy density, has stood out from various energy alternatives and is believed to be the ideal renewable energy carrier for the future.[1-5] Since there is no natural resource, hydrogen is usually produced through various chemical reactions, such as steam reforming of natural gas or coal, which will produce greenhouse gas during the synthesis. Water electrolysis using electrical power as generated from renewable energies, such as solar and wind, as the energy input, is one of the most attractive ways for mass production of hydrogen, because of its true zero-emission nature.[6, 7]

Similar to many other electrochemical reactions, electrochemical hydrogen generation (hydrogen evolution reaction, HER) occurring at the cathode of a water splitting cell is subjected to kinetics barriers. To promote the HER process with reduced overpotential, an energetic electrocatalyst is thus required.[8, 9] As the state-of-the-art HER electrocatalysts, Platinum (Pt)-group noble metals are characterized by high activity, but also show the disadvantages of scarcity, high price and insufficient durability.[9-13] More recently, metal nitride/phosphide/sulfide have been extensively applied as the alternative HER electrocatalysts, showing outstanding activity.[14-18] Considering the similar electronic structure of the other noble metal elements to Pt, the

formation of noble metal phosphides has also been extensively exploited to fine tune the electronic structure of the noble metal, so as to realize the HER activity similar or even outperforming that of Pt.[19-23] For example, Ru_2P and RuP nanostructures were found to show HER activity exceeding that of Pt catalyst under alkaline electrolyte. However, due to the hurdle reaction conditions for electrochemical water splitting process (either alkaline or acidic solution is applied as the electrolyte), the oxidation or dissolution/corrosion of such precious metals and metal nitride/phosphide/sulfide materials in/by the electrolyte solution is a big concern, which may cause significant performance decay with time on operation. For example, nanosized RuP was unstable with respect to ambient air and moisture, and it was oxidized by exposure to air with the formation of RuO_2, which is easily dissolved by the liquid electrolyte, resulting in poor durability.[23] In order to suppress the corrosion by the electrolyte, large size electrocatalysts have to be made. In addition, such metal phosphides are usually semiconductors with poor electric conductivity, requiring carbon additive to improve the charge transfer efficiency.

As compared to the easy corrosion by the liquid electrolyte of oxides and sulfide/nitride/phosphides, many carbon materials show favorable corrosion resistance toward the electrolyte solutions. Unfortunately, most of pure carbon materials still show inferior activity to precious metal and metal nitride/phosphide/sulfides. The formation of core-shell nanostructured materials with a metal or metal-P, S, N core and carbon or doped carbon shell is a new way to develop alternative HER electrocatalysts.[24-26] Two obvious beneficial effects can be derived from such unique nanostructured catalyst

architecture. First, the apparent conductivity can be significantly improved due to the carbon coating, resulting in improved charge transfer process. Second, the carbon shell effectively avoids the direct contact of the metallic core with the liquid electrolyte; consequently, the dissolution problem of many metal or metal oxides/phosphides/nitrides/sulfides nanoparticles can be effectively suppressed or avoided. The metals or metal oxides/phosphides/nitrides/sulfides core can strongly interact with the carbon shell, which can cause a change of the electronic structure of the shell, consequently enhancing the activity of the carbon for HER. Recently we have demonstrated that $Co_{1-x}Ru_xP$/nitrogen and phosphorus doped carbon (NPC) nanostructure showed comparable activity for HER to Pt/C precious metal catalyst in a wide pH value of liquid electrolyte.[27] Such improved performance was also partially resulted from the reduced particle size of the $Co_{1-x}Ru_xP$ phase, while the NPC shell prevent the oxidation of the core, thus ensuring high stability. In that study, Ru was used to fine tune the electronic structure of the cobalt phosphide core as well.

As we know, different noble metals have slightly different electronic structure. A systematic study of noble-metal phosphide/NPC composites for HER will provide useful information about how the noble metal affects the performance of metal/carbon composite, and thus provides guidance for the design of novel noble metal-based metal phosphide/carbon or noble metal-doped metal phosphide/carbon composite as efficient HER electrocatalysts.

Herein, we reported the synthesis of various noble-metal phosphides (RhP_2, RuP_2,

PtP_2, IrP_2 and Pd_5P_2) nanoparticles wrapped by ultrathin N, P-codoped graphitic carbon shells (MP_x@NPGC, MP_x=RhP_2, RuP_2, PtP_2, IrP_2 and Pd_5P_2) via a recent demonstrated synthetic process,[35] and comprehensive investigation about the core effect of different noble-metal phosphides, primarily on the HER performance in both acidic and alkaline electrolytes, was conducted. Based on the physical characterization and electrochemical analysis, the catalytic properties of MP_x@NPGC were found to be largely depended on the intrinsic activities of the noble-metal phosphides core. Among them, the RhP_2@NPGC exhibited the highest HER activity with a small overpotential of 78 mV to motivate the hydrogen production at the current density of 10 mA cm^{-2} (η_{10}) and a low Tafel slope of 43 mV dec^{-1} in 0.5 M H_2SO_4 solution, while the highest-performance catalysts among them in the 1 M KOH medium was RuP_2@NPGC with η_{10} of 108 mV and a small Tafel slope of 30 mV dec^{-1}. In addition, all samples possessed favorable long-term operation stability. Consequently, this study offers new insights to fabricate novel nanostructured electrocatalysts with enhanced performance.

2. RESULTS AND DISCUSSION

Figure 1 depicted the general synthesis procedure of the various MP_x@NPGC core-shell structured hybrids, which involves two subsequent steps of homogeneous mixing and simple annealing treatment under argon gas flow with the experimental details given in the **Experimental section**. During the pyrolysis process, the carbonization and phosphidation of precursors occurred simultaneously with the formation of the targeted core-shell structured products.[16] The room-temperature X-ray diffraction (XRD) patterns of the samples using different noble-metal chloride salts

($RhCl_3$, $RuCl_3$, H_2PtCl_6, $IrCl_3$) as the raw materials, as shown in **Figure 1**, matched well correspondingly with the standard diffraction cards of crystalline phases of RhP_2 (JCPDS-65-1272), RuP_2 (JCPDS-34-0333), PtP_2 (JCPDS-80-2220) and IrP_2 (JCPDS-89-3985) (The detailed description for XRD patterns are shown in the **Supporting Information**). Thus, these samples are denoted as RhP_2@NPGC, RuP_2@NPGC, PtP_2@NPGC and IrP_2@NPGC, respectively. The similar molecular composition of the core, i.e., MP_2, makes them reasonable comparison for the HER activity, which will be discussed later. The only exception is the palladium case. By using $PdCl_2$ as the raw material, the as-formed MP_x phase was found to be Pd_5P_2 (JCPDS-19-0887). Even with more phosphorus source involved, Pd_5P_2 phase structure remained unchanged (**Figure S1**), suggesting the preferentially stable existence of Pd_5P_2 among the various palladium phosphides (Pd_xP_y). In addition to the metal phosphide phase, N, P co-doped carbon was also formed, which was confirmed by our previous study, [27] and will be discussed later.

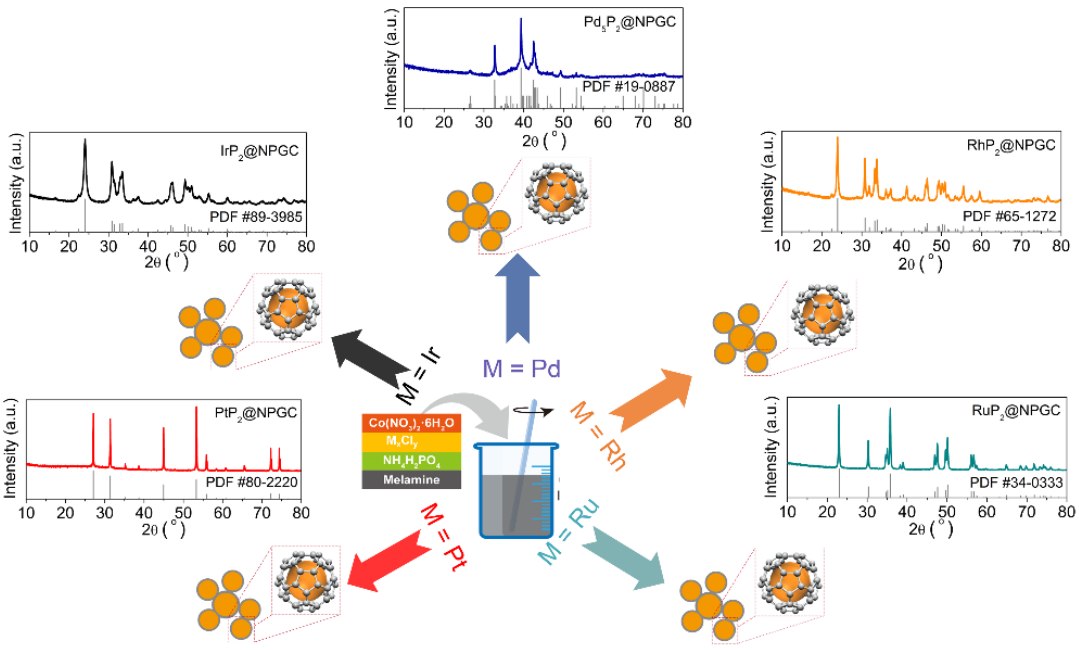

Figure 1. The general synthesis procedure of MP_x@NPGC and corresponding XRD patterns.

To understand the effect of different cores in the core-shell structures on the HER activity, the HER catalytic properties of all the as-synthesized MP_x@NPGC samples were firstly comparatively evaluated in both 1 M KOH and 0.5 M H_2SO_4 electrolytes. As references, the HER activity of commercial Pt/C catalyst and the pristine N, P co-doped graphitic carbon (NPGC) (synthesized without the application of precious metal chloride) was also measured under the similar conditions. **Figure 2a** & **c** displayed the typical IR-corrected polarization curves of all the investigated core-shell structured catalysts and the reference samples (Pt/C, NPGC), taken on the glassy carbon (GC) electrode. Among the various MP_x@NPGC core-shell nanostructured hybrids, in the acidic medium (0.5 M H_2SO_4), the RhP_2@NPGC hybrid afforded the highest HER activity with the smallest initial overpotential, followed by Pd_5P_2@NPGC, and then RuP_2@NPGC and IrP_2@NPGC, while the PtP_2@NPGC sample showed the lowest activity. Specifically, the overpotentials required to reach the representative current density of 10 mA cm^{-2} (η_{10}) are 78, 128, 158, 149, and 104 mV for the RhP_2@NPGC, RuP_2@NPGC, PtP_2@NPGC, IrP_2@NPGC, and Pd_5P_2@NPGC hybrids, respectively. Notably, although the RuP_2@NPGC sample exhibited inferior HER performance than the Pd_5P_2@NPGC hybrid in terms of η_{10}, the RuP_2@NPGC outperformed Pd_5P_2@NPGC with the higher current densities when the overpotential is larger than 149 mV, which reveal that RuP_2@NPGC possessed the faster reaction kinetics at the high overpotential range. In comparison, the pure NPGC carbon material showed negligible HER activity. It suggests the metal phosphides core in the hybrids strongly

affect the NPGC shell's electronic structure, making the NPGC shell to demonstrate significantly improved HER activity as compare to the bare NPGC. It is highly attractive that the RhP_2@NPGC among these five samples has closest HER activity to the benchmark Pt/C catalyst. As illustrated in **Figure 2b**, the Tafel plots of all the samples were constructed to disclose their catalytic kinetics, and the Tafel slopes of 43, 44, 66, 62, 62, 139 and 27 mV dec^{-1} were derived for RhP_2@NPGC, RuP_2@NPGC, PtP_2@NPGC, IrP_2@NPGC, Pd_5P_2@NPGC, NPGC and Pt/C, respectively. Here, a lower Tafel slope obtained for the RhP_2@NPGC hybrid than the other MP_x@NPGC hybrid catalysts is an important indication of the faster catalytic rate of the former. When the alkaline electrolyte was used, a different HER-activity trend among the above-mentioned catalysts was observed. Among the various MP_x@NPGC hybrids, RuP_2@NPGC became the most active catalyst. The η_{10} increased in the order of Pt/C (25 mV) < RuP_2@NPGC (108 mV) < RhP_2@NPGC (170 mV) < PtP_2@NPGC (214 mV) < IrP_2@NPGC (263 mV) < Pd_5P_2@NPGC (397 mV) < NPGC (538 mV). In addition, among the various hybrids, the RuP_2@NPGC hybrid presented the lowest Tafel slope of 30 mV dec^{-1}, which is even smaller than Pt/C (**Figure 2d**), revealing its superior HER kinetics. In addition to the HER activity, durability is another key indicator of an HER electrocatalyst targeting practical applications. Galvanostatic tests at the current density of 10 mA cm^{-2} were first performed to evaluate the stability. According to **Figure 2e &f**, the applied potential values for all the investigated MP_x@NPGC hybrids displayed a little increase after 8 h of continuous hydrogen generation, specially under alkaline conditions, but still demonstrating their moderate

operating stability. The carbon shell can effectively avoid the direct contact of metal phosphide with the liquid electrolyte that contributes to such operating stability of the hybrids. Besides, time-dependent current density curves of these MP_x@NPGC hybrids in acidic condition were also observed (**Figure S2**), further confirming the moderate stability.

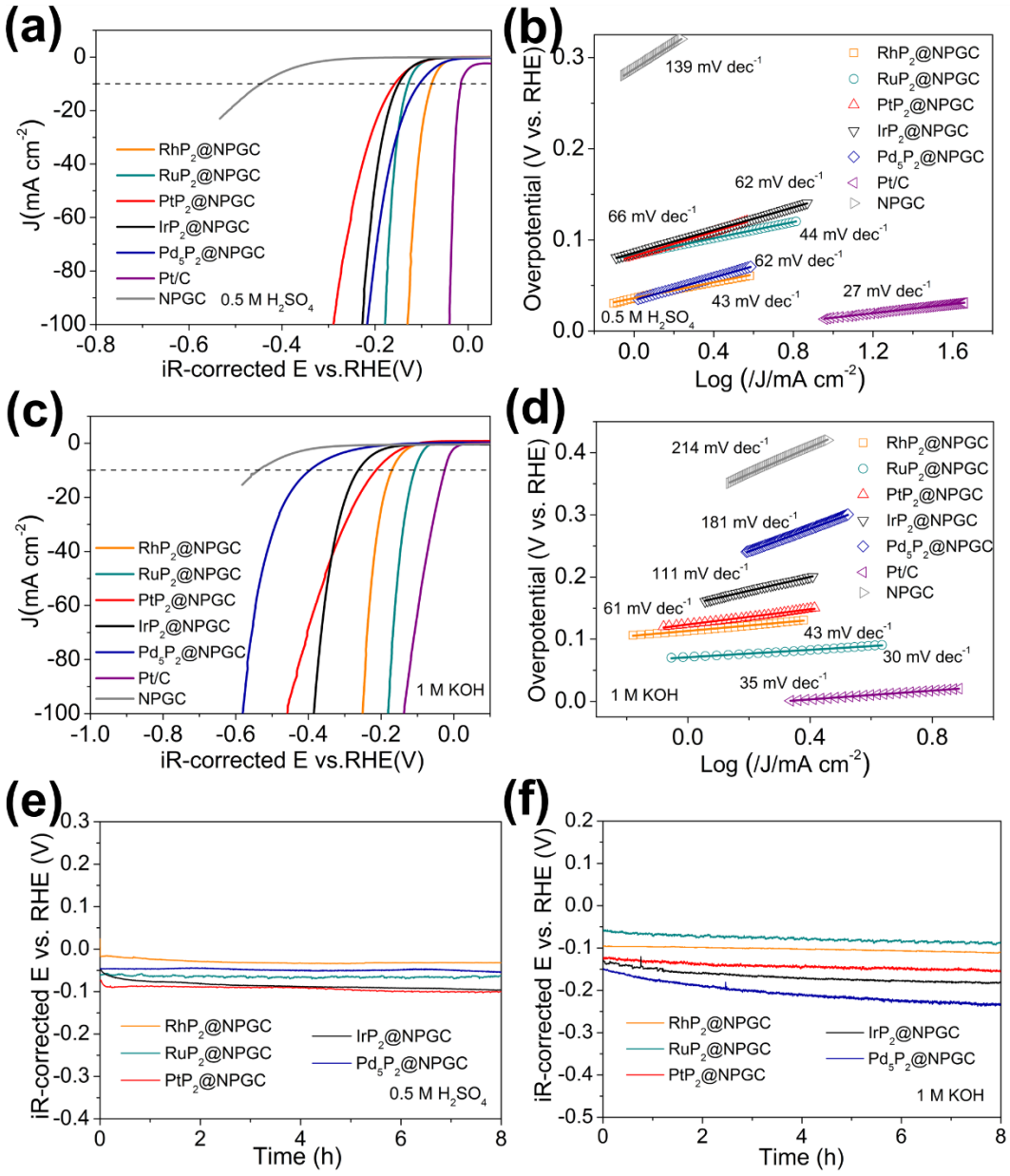

Figure 2. (a, c) HER polarization curves and (b, d) the corresponding Tafel plots of these MP_x@NPGC samples, NPGC and commercial 20 % Pt/C catalyst in 0.5 M H_2SO_4 (a, b) and 1 M KOH (c, d) electrolytes. (e, f) Galvanostatic tests at the current density of 10 mA cm^{-2} for five

MP_x@NPGC catalysts loaded on carbon cloth in both (e) acidic and (f) alkaline media.

As it is well known, for the core-shell structured electrocatalysts, the activity is mainly contributed by the shell while the core inputs its effect by altering the electronic structure of the shell. To understand the origin of the different HER activity of the various MP_x@NPGC hybrids, their morphology and microstructure were first examined. According to the field-emission scanning electron microscopy (FESEM) images as shown in **Figure S3**, all the samples had irregular particulate shape with different sizes. The IrP_2@NPGC hybrid showed the smallest particle size, while the PtP_2@NPGC hybrid presented the largest particle size. Closer observation was disclosed by the corresponding Transmission electron microscopy (TEM). As shown in **Figure 3a-e,** these metal phosphide nanoparticles with the diameters ranging from 5 to 100 nm were uniformly encapsulated in ultrathin carbon layer. In high-resolution transmission electron microscopy (HR-TEM) images, well-resolved lattice spacings of 0.209, 0.386, 0.201, 0.240, and 0.228 nm are observed, which are in well agreement with the distances of the RhP_2 (102), RuP_2 (110), PtP_2 (220), IrP_2 (-202), and Pd_5P_2 (-113) facets, respectively. The homogeneous element distribution of metal (Rh, Ru, Pt, Ir, and Pd), and phosphorus were also observed within the selected matrix. According to the inductively coupled plasma atom emission spectrometry (ICP-AES) results, the metal content was found to be around 42.6, 58.1, 41.5, 62.6, and 56.5 wt. % for the RhP_2@NPGC, RuP_2@NPGC, PtP_2@NPGC, IrP_2@NPGC, and Pd_5P_2@NPGC hybrids, respectively. Besides, in order to reveal the morphology and phase structure of the samples after testing, the SEM image and XRD pattern of the post-HER RhP_2@NPGC

catalyst were shown in **Figure S4**, indicating that the micro-morphology and phase structure were well maintained.

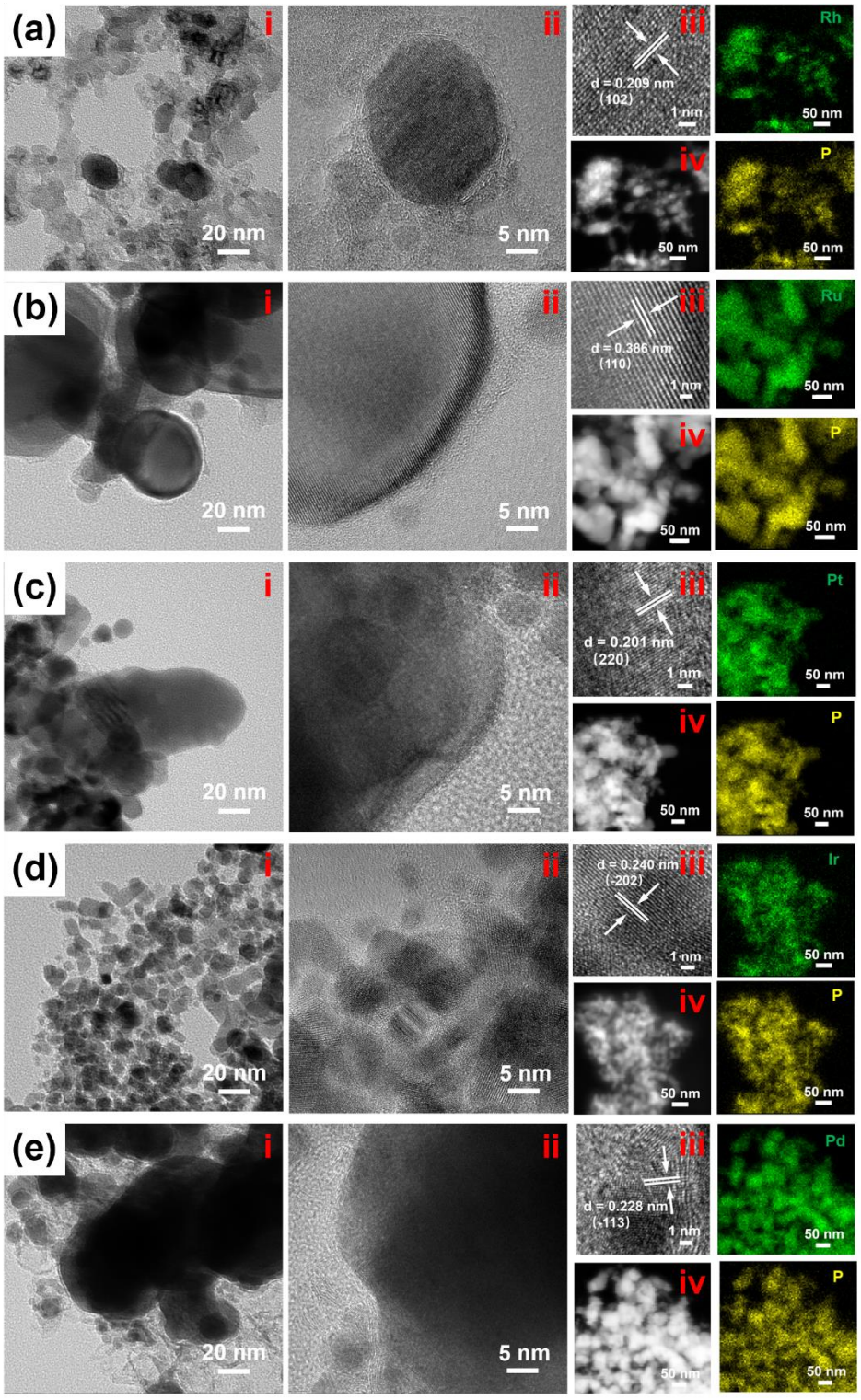

Figure 3. (a-e) TEM (i) and HR-TEM images (ii, iii), and the corresponding energy-dispersive X-ray spectroscopy (EDS) elemental mappings (iv) of MP_x@NPGC samples ((a) RhP_2@NPGC, (b) RuP_2@NPGC, (c) PtP_2@NPGC, (d) IrP_2@NPGC, and (e) Pd_5P_2@NPGC).

X-ray photoelectron spectroscopy (XPS) analysis was performed to probe the chemical compositions and valence states of the various elements in all the MP_x@NPGC hybrids. Shown in **Figure S5** are the overview survey spectra, indicating the presence of metals (Rh, Ru, Pt, Ir, and Pd), P, N, and C. In the RhP_2@NPGC hybrid, the high-resolution Rh 3d spectrum displayed the main peaks at 308.5 and 313.2 eV, which were attributed to Rh $3d_{5/2}$ and Rh $3d_{3/2}$, respectively (**Figure 4a**). They were well above the value for metallic Rh (~307.5 eV in the Rh $3d_{5/2}$ region) and slightly below that of Ru^{3+}(~308.8 eV in the Rh $3d_{5/2}$ region), demonstrating that Rh atom in RhP_2 was partially positive charged ($Rh^{\delta+}$).[28] For the fitted P 2p region, there were four peaks at 129.5, 130.3, 132.2, and 133.9 eV, corresponding to the P $2p_{3/2}$, P $2p_{1/2}$, P-C bonds, and the phosphate species (P-O), respectively (**Figure 4b**).[27] The lower binding energy of P 2p3/2 for phosphide relative to elemental P suggested the P in RhP_2 holds a slightly negative charge ($P^{\delta-}$). As depicted in **Figure 4c**, the high-resolution N 1s spectrum was fitted into four types of nitrogen environments located at 398.8, 401, 401.9, and 404.1 eV, which agreed well with the pyridinic N, pyrrolic N, graphitic N, and oxygenated N, respectively.[29] Similarly, M-P bonding or N species were also obtained in the other MP_x@NPGC hybrids with the results presented in **Figure S6 and S7**. It suggests the N is mainly formed bond with carbon, and the P formed bonds with both the metal element and carbon. It further confirms the MP_x structure of the core and N/P co-doped carbon structure of the shell. Besides, the XPS data for NPGC were also presented in **Figure S8** and the observed N species or P species confirmed the successful doping of N and P, matching well with the XPS results in MP_x@NPGC

hybrids.

To detect the properties of the carbon shell, Raman spectra results were presented in **Figure 4d.** Typically, D and G bands situated at about 1342 and 1685 cm^{-1} represented the defects on the disordered carbon and the graphitic structure, respectively. The intensity ratios (I_D/I_G) for these five catalysts were all similar, within the range of 1.01-1.07, revealing the similar carbon structure with partial graphitization and abundant defects; hence, it was favorable to both electron conduction and H^+/H_2 absorption.[30, 31] The N_2 adsorption-desorption isotherms in **Figure S9** showed a type-II isotherm along with a H_3-type hysteresis loop for all samples, suggesting the presence of mesopores. The specific surface areas of RhP_2@NPGC, RuP_2@NPGC, PtP_2@NPGC, IrP_2@NPGC and Pd_5P_2@NPGC, calculated based on the BET method from the N_2 adsorption-desorption isotherms, are 78.6, 29.6, 10.9, 85.1 and 24.5 $m^2\ g^{-1}$, respectively. Meanwhile, the total pore volumes of RhP_2@NPGC, RuP_2@NPGC, PtP_2@NPGC, IrP_2@NPGC, and Pd_5P_2@NPGC are 0.29, 0.10, 0.05, 0.33 and 0.08 $cm^3\ g^{-1}$, respectively. These values are listed in **Table S1.**

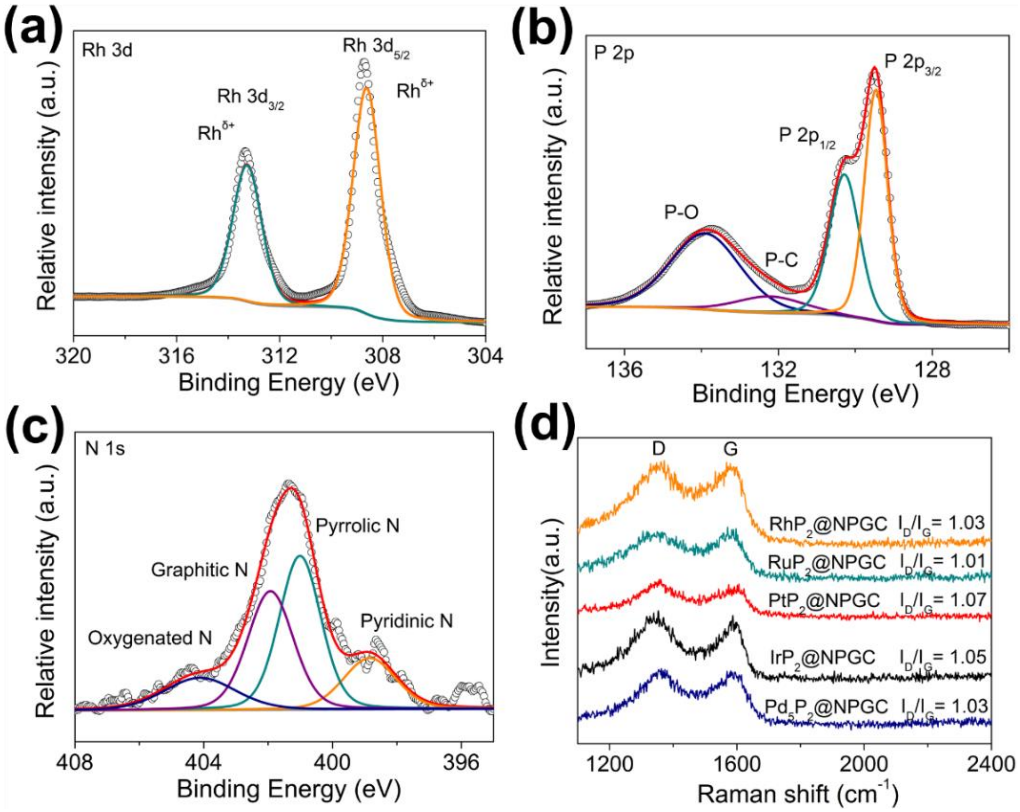

Figure 4. (a-c) High-resolution XPS spectra of Rh 3p (a), P 2p (b), and N 1s (c) of the as-obtained RhP_2@NPGC. (d) Raman spectra of MP_x@NPGC samples.

According to previous studies, the favorable microstructure features such as large BET specific area, small particle size, abundant pores, high graphitic carbon, and rich carbon defects, etc., are closely correlated with the excellent electrocatalytic performance.[5, 6, 8, 12, 30, 21] Clearly, no direct relation between the activity and the microstructure properties for the current MP_x@NPGC hybrids was demonstrated. For example, in 0.5 M H_2SO_4 and 1 M KOH electrolyte solutions, the RhP_2@NPGC hybrid and the RuP_2@NPGC hybrid showed the best performance, respectively, while both of them did not showed the highest surface area or the smallest particle size. It suggests the different HER performance of the various MP_x@NPGC hybrid catalysts is more likely originated from their different metal phosphide cores.

To exclude the morphology effect on the performance, the intrinsic activity of the different samples was exploited. We first determined the electrochemically active surface area (ECSA) to explore active sites, which is linearly related to the electrochemical double-layer capacitance (C_{dl}). To obtain C_{dl} values, the cyclic voltammograms (CVs) with different scan rates were tested, as displayed in **Figure S10** and **Figure S11** for all the MP_x@NPGC hybrids. **Figure 5a&b** presented the calculated C_{dl} values for these catalysts; when assuming 40 μF cm^{-2} as the specific capacitance, the specific ECSA results were obtained and listed in **Table S2**.[32] In general, the larger ECSAs mean more catalytically active sites, so that to enhance the apparent catalytic activity.[32] Yet, the obvious mismatch between ECSA results and the HER activities further confirmed that the metal phosphides core played an important role in determining the HER activity of the hybrid catalyst with similar carbon shell. By normalizing to ECSA values, the intrinsic activities for MP_x@NPGC hybrids in both alkaline and acid media were derived. As shown in **Figure 5c** and **d**, in the acidic medium and at -0.1 V, the RhP_2@NPGC hybrid showed a specific current density of 0.21 mA cm_{ECSA}^{-2}, which is about 5.2-, 1.2-, 14-, and 1.6-fold that of the RuP_2@NPGC (0.04 mA cm_{ECSA}^{-2}), PtP_2@NPGC (0.18 mA cm_{ECSA}^{-2}), IrP_2@NPGC (0.015 mA cm_{ECSA}^{-2}), and Pd_5P_2@NPGC (0.13 mA cm_{ECSA}^{-2}). In the alkaline medium, the specific current densities at -0.1 V were increased in the trend of Pd_5P_2@NPGC < IrP_2@NPGC < RhP_2@NPGC < PtP_2@NPGC < RuP_2@NPGC. To investigate the electrode kinetics during the HER process, we also carried out electrochemical impedance spectroscopy (EIS) measurements at the potential of -0.4 and -1.2 V vs. Ag/AgCl for a series of

MP_x@NPGC catalysts. As can be seen from **Figure S12**, RhP_2@NPGC and RuP_2@NPGC among these hybrids displayed the smallest charge transfer resistance (R_{ct}) values in the EIS in 0.5 M H_2SO_4 and 1 M KOH, respectively, implying much faster charge transfer and surface reaction rates for the HER process, which could also contribute to the enhanced catalytic activities.[32]

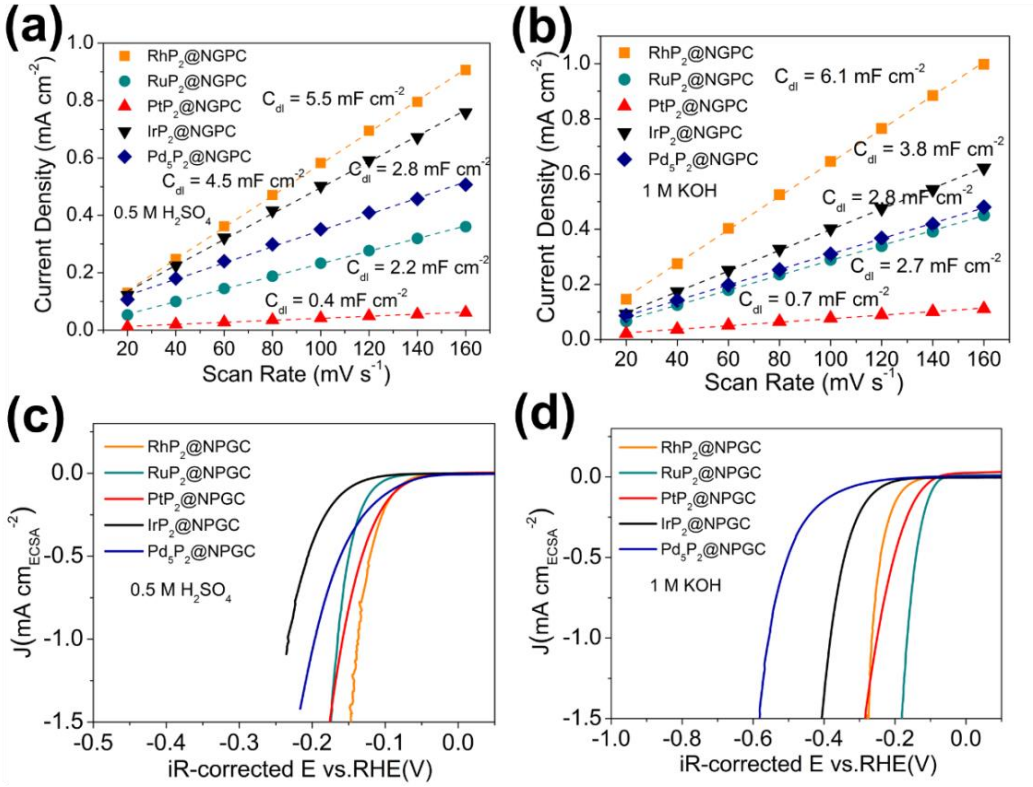

Figure 5. (a, b) The linear fitting plots of the capacitive currents versus scan rates from **Figure S7** and **Figure S8** for MP_x@NPGC samples in acidic (a) and alkaline (b) media, respectively. (c, d) HER polarization curves normalized by ECSA for MP_x@NPGC samples in acidic (c) and alkaline (d) media, respectively.

For HER, there are two possible mechanisms, i.e., Volmer-Heyrovsky and Volmer-Tafel process, [33] as follows:

In acidic electrolyte:

$$\text{Volmer step: } * + H^+ + e^- \rightarrow H* \qquad (1)$$

Heyrovsky step: $H* + H^+ + e^- \rightarrow * + H_2$ (2)

Tafel step: $2H* \rightarrow 2* + H_2$ (3)

In alkaline electrolyte:

Volmer step: $* + H_2O + e^- \rightarrow H* + OH^-$ (4)

Heyrovsky step: $H* + H_2O + e^- \rightarrow * + H_2 + OH^-$ (5)

Tafel step: $2H* \rightarrow 2* + H_2$ (6)

Above reactions clearly show that the reaction intermediate of H* was involved during the HER process. The binding strength between a catalyst surface and the reaction intermediates are critical for the electrocatalysis of HER. For example, the Gibbs free energy of hydrogen adsorption (ΔG_{H*}) is usually used as an activity descriptor for HER. The reaction intermediate binding strength for a good catalyst should not to be too strong or too weak, i.e., ΔG_{H*} is close to 0.[23] For carbon-based electrocatalysts, the adsorption of intermediates could be adjusted by heteroatom doping, defects/edge modification, and surface functionalization, etc.[34] Clearly, the metal phosphide core also caused influence on the electronic structure of the carbon shell, thus altered its Gibbs free energy of hydrogen adsorption. As demonstrated by XPS, different metal phosphides showed different apparent oxidation states and electronic structure. Due to the strong coupling effect, some electrons belonging to metallic core were transferred to the outer carbon shell, thus significantly altering the electronic properties of the carbon shell, which has been confirmed by previous similar

studies.[12, 36] For the different metallic cores, the electron transfer numbers from encapsulated metals to carbon shell surface is largely different, but the specific values are difficult to be obtained, only by more advanced characterizations and possible DFT calculations.[35, 37] In order to further confirm the strong coupling effect between the metal phosphides and carbon shell on the HER activity trend, some control experiments were conducted. As shown in **Figure S13**, the pure metal phosphides performed poor HER activity in both acidic and alkaline conditions, and the physical mixture of different metal phosphides and graphene showed the similar activity trend with that of pure metal phosphides, but which are superior to pure metal phosphides, indicating that the graphene might enhance the conductivity of mixture and thus help to improve their activity. Besides, MP_x@NPGC are more active than the physical mixture for hydrogen generation, and the activity trend of MP_x@NPGC is obviously different from pure metal phosphides or the physical mixture, convectively suggesting that the different HER activities for various MP_x@NPGC were attributed to the strong coupling effect from core-shell structure. As well, based on the electrocatalysis results, the pH value of the electrolyte likely also introduced important effect on the adsorption energy of hydrogen over the carbon surface, thus different active trends of the various hybrids in acidic and alkaline electrolyte solutions were observed.

3. CONCLUSIONS

In summary, a comparative study of HER catalytic performance for the core-shell structured noble-metal phosphides-based electrocatalysts in both acidic and alkaline media was presented for the first time. The apparent HER activity for these

MP_x@NPGC samples increased in the order of PtP_2@NPGC < IrP_2@NPGC < RuP_2@NPGC < Pd_5P_2@NPGC < RhP_2@NPGC in 0.5 M H_2SO_4, and Pd_5P_2@NPGC < IrP_2@NPGC < PtP_2@NPGC < RhP_2@NPGC < RuP_2@NPGC in 1 M KOH. After being normalized by ECSA, the RhP_2@NPGC and RuP_2@NPGC still exhibited the most excellent HER activities in acidic and alkaline solutions, respectively. Combining with the various characterization analysis, the HER activities of MP_x@NPGC were found to be closely associated with the noble-metal phosphide cores and the pH value of the electrolyte solution. It suggests the simultaneous modification of the functional core as well as the liquid electrolyte is recommended to optimize the core-shell structured electrocatalyst for HER. These findings then provide useful guidance for the future design of other core-shell structured electrocatalysts for HER, which should also be applicable for other electrochemical reaction such as oxygen evolution reaction and oxygen reduction reaction.

ASSOCIATED CONTENT

Supporting Information

The Supporting Information is available free of charge on the ACS Publications website. Experimental section (including the detail materials synthesis process), various characterization results (XRD, SEM, XPS, and BET), and HER electrochemical data.

AUTHOR INFORMATION

Corresponding Author

*E-mail: zhouwei1982@njtech.edu.cn (Wei Zhou). Tel.: +86 25 83172256; Fax: +86 25 83172242.

*E-mail: shaozp@njtech.edu.cn (Zongping Shao). Tel.: +86 25 83172256; Fax: +86 25 83172242.

Notes

The authors declare no competing financial interest.

ACKNOWLEDGMENTS

This meaningful study was financially supported by the Jiangsu Natural Science Foundation for Distinguished Young Scholars (No. BK20170043), the National Nature Science Foundation of China (No. 21576135), the Youth Fund in Jiangsu Province (No. BK20150945), and the Program for Changjiang Scholars.

REFERENCES

(1) Lin, L.; Zhou, W.; Gao, R.; Yao, S.; Zhang, X.; Xu, W.; Zheng, S.; Jiang, Z.; Yu, Q.; Li, Y.-W.; Shi, C.; Wen, X.-D.; Ma, D. Low-temperature hydrogen production from water and methanol using Pt/alpha-MoC catalysts. *Nature* **2017**, *544*, 80-83.

(2) Subbaraman, R.; Tripkovic, D.; Strmcnik, D.; Chang, K.-C.; Uchimura, M.; Paulikas, A. P.; Stamenkovic, V.; Markovic, N. M. Enhancing hydrogen evolution activity in water splitting by tailoring Li^+-$Ni(OH)_2$-Pt interfaces. *Science* **2011**, *334*, 1256-1260.

(3) Zou, X.; Zhang, Y. Noble metal-free hydrogen evolution catalysts for water splitting. *Chem. Soc. Rev.* **2015**, *44*, 5148-5180.

(4) Zhang, L.; Jia, Y.; Gao, G.; Yan, X.; Chen, N.; Chen, J.; Soo, M. T.; Wood, B.; Yang, D.; Du, A.; Yao, X. Graphene defects trap atomic Ni species for hydrogen and oxygen evolution reactions.

Chem **2018**, *4*, 285-297.

(5) Yu, J.; Zhong, Y.; Zhou, W.; Shao, Z. Facile synthesis of nitrogen-doped carbon nanotubes encapsulating nickel cobalt alloys 3D networks for oxygen evolution reaction in an alkaline solution. *J. Power Sources* **2017**, *338*, 26-33.

(6) Fang, Z.; Peng, L.; Qian, Y.; Zhang, X.; Xie, Y.; Cha, J. J.; Yu, G. Dual Tuning of Ni-Co-A (A = P, Se, O) Nanosheets by anion substitution and holey engineering for efficient hydrogen evolution. *J. Am. Chem. Soc.* **2018**, *140*, 5241-5247.

(7) Zhang, Z.; Li, P.; Feng, Q.; Wei, B.; Deng, C.; Fan, J.; Li, H.; Wang, H. Scalable synthesis of ruthenium-based electrocatalyst as a promising alternative to Pt for hydrogen evolution reaction. *ACS Appl. Mater.& Interfaces* **2018**, *10*, 32171-32179.

(8) Wang, M.-Q.; Ye, C.; Liu, H.; Xu, M.; Bao, S.-J. Nanosized metal phosphides embedded in nitrogen-doped porous carbon nanofibers for enhanced hydrogen evolution at all pH values. *Angew. Chem. Int. Ed.* **2018**, *57*, 1963-1967.

(9) Zeng, X.; Shui, J.; Liu, X.; Liu, Q.; Li, Y.; Shang, J.; Zheng, L.; Yu, R. Single-atom to single-atom grafting of Pt_1 onto Fe-N_4 center: Pt_1@Fe-N-C multifunctional electrocatalyst with significantly enhanced properties. *Adv. Energy Mater.* **2018**, *8*, 1701345.

(10) Cao, Z.; Chen, Q.; Zhang, J.; Li, H.; Jiang, Y.; Shen, S.; Fu, G.; Lu, B.-a.; Xie, Z.; Zheng, L. Platinum-nickel alloy excavated nano-multipods with hexagonal close-packed structure and superior activity towards hydrogen evolution reaction. *Nat. Commun.* **2017**, *8*, 15131.

(11) Mahmood, J.; Li, F.; Jung, S.-M.; Okyay, M. S.; Ahmad, I.; Kim, S.-J.; Park, N.; Jeong, H. Y.; Baek, J.-B. An efficient and pH-universal ruthenium-based catalyst for the hydrogen evolution reaction. *Nature Nanotechnol.* **2017**, *12*, 441-446.

(12) Su, J.; Yang, Y.; Xia, G.; Chen, J.; Jiang, P.; Chen, Q. Ruthenium-cobalt nanoalloys encapsulated in nitrogen-doped graphene as active electrocatalysts for producing hydrogen in alkaline media. *Nat. Commun.* **2017**, *8*, 14969.

(13) Wang, P.; Zhang, X.; Zhang, J.; Wan, S.; Guo, S.; Lu, G.; Yao, J.; Huang, X. Precise tuning in platinum-nickel/ nickel sulfide interface nanowires for synergistic hydrogen evolution catalysis. *Nat. Commun.* **2017**, *8*, 14580.

(14) Mahmood N.; Yao Y.; Zhang, J.; Pan L.; Zhang X.; Zou J. Electrocatalysts for hydrogen evolution in alkaline electrolytes: mechanisms, challenges, and prospective solutions. *Adv. Sci.* **2018**, *5*, 1700464.

(15) Shi, Y.; Zhang, B. Recent advances in transition metal phosphide nanomaterials: synthesis and applications in hydrogen evolution reaction. *Chem. Soc. Rev.* **2016**, *45*, 1529-1541.

(16) Pu, Z.; Zhang, C.; Amiinu, I. S.; Li, W.; Wu, L.; Mu, S. General strategy for the synthesis of transition-metal phosphide/N-doped carbon frameworks for hydrogen and oxygen evolution. *ACS Appl. Mater. Interfaces* **2017**, *9*, 16187-16193.

(17) Zhang, C.; Shi, Y.; Yu, Y.; Du, Y.; Zhang, B. Engineering sulfur defects, atomic thickness, and porous structures into cobalt sulfide nanosheets for efficient electrocatalytic alkaline hydrogen evolution. *ACS Catal.* **2018**, *8*, 8077-8083.

(18) Lai, J.; Huang, B.; Chao, Y.; Chen, X.; Guo, S. Strongly coupled nickel–cobalt nitrides/carbon hybrid nanocages with Pt‐like activity for hydrogen evolution catalysis. *Adv. Mater.* **2019**, 11, 1805541.

(19) Duan, H.; Li, D.; Yan, T.; Yang, H.; Ji, S. F.; Wang, R.; Lv, H.; Lopes, P. P.; Paulikas, A. P.; Li, H. High performance Rh_2P electrocatalyst for efficient water splitting. *J. Am. Chem. Soc.* **2017**, *139*,

5494-5502.

(20) Pu, Z.; Amiinu, I. S.; Kou, Z.; Li, W.; Mu, S. RuP_2-based catalysts with platinum-like activity and higher durability for the hydrogen evolution reaction at all pH values. *Angew. Chem. Int. Ed.* **2017**, *56*, 11717-11722.

(21) Liu, T.; Wang, S.; Zhang, Q.; Chen, L.; Hu, W.; Li, C. M. Ultrasmall Ru_2P nanoparticles on graphene: a highly efficient hydrogen evolution reaction electrocatalyst in both acidic and alkaline media. *Chem. Commun.* **2018**, *54*, 3343-3346.

(22) Yang, F.; Zhao, Y.; Du, Y.; Chen, Y.; Cheng, G.; Chen, S.; Luo, W. A Monodisperse Rh_2P-based electrocatalyst for highly efficient and pH-universal hydrogen evolution reaction. *Adv. Energy Mater.* **2018**, *8*, 1703489.

(23) Yu, J.; Guo, Y.; She, S.; Miao, S.; Ni, M.; Zhou, W.; Liu, M.; Shao, Z. Bigger is surprisingly better: agglomerates of larger RuP nanoparticles outperform benchmark Pt nanocatalysts for the hydrogen evolution reaction. *Adv. Mater.* **2018**, *30*, 1800047.

(24) Das, D.; Nanda, K. K. One-step, integrated fabrication of Co_2P nanoparticles encapsulated N, P dual-doped CNTs for highly advanced total water splitting. *Nano Energy* **2016**, *30*, 303-311.

(25) Cao, Y.; Meng, Y.; Huang, S.; He, S.; Li, X.; Tong, S.; Wu, M. Nitrogen-, oxygen- and sulfur-doped carbon-encapsulated Ni_3S_2 and NiS core-shell architectures: bifunctional electrocatalysts for hydrogen evolution and oxygen reduction reactions. *ACS Sustainable Chem. Eng.* **2018**, *6*, 15582-15590.

(26) Wang, M.; Tang, C.; Ye, C.; Duan, J.; Li, C.; Chen, Y.; Bao, S.; Xu, M. Engineering the nanostructure of molybdenum nitride nanodot embedded N-doped porous hollow carbon nanochains for rapid all pH hydrogen evolution. *J. Mater. Chem. A* **2018**, *6*, 14734-14741.

(27) Yu, J.; Wu, X.; Zhong, Y.; Yang, G.; Ni, M.; Zhou, W.; Shao, Z. Multifold nanostructuring and atomic-scale modulation of cobalt phosphide to significantly boost hydrogen production. *Chem. Eur. J.* **2018**, *24*, 13800-13806.

(28) Wang, K.; Huang, B.; Lin, F.; Lv, F.; Luo, M.; Zhou, P.; Liu, Q.; Zhang, W.; Yang, C.; Tang, Y.; Yang, Y.; Wang, W.; Wang, H.; Guo, S. Wrinkled Rh_2P nanosheets as superior pH-universal electrocatalysts for hydrogen evolution catalysis. *Adv. Energy Mater.* **2018**, *8*, 1801891.

(29) Li, J.; Song, Y.; Zhang, G.; Liu, H.; Wang, Y.; Sun, S.; Guo, X. Pyrolysis of self-assembled iron porphyrin on carbon black as core/shell structured electrocatalysts for highly efficient oxygen reduction in both alkaline and acidic medium. *Adv. Funct. Mater.* **2017**, *27*, 1604356.

(30) Ma, Y.-Y.; Wu, C.-X.; Feng, X.-J.; Tan, H.-Q.; Yan, L.-K.; Liu, Y.; Kang, Z.-H.; Wang, E.-B.; Li, Y.-G. Highly efficient hydrogen evolution from seawater by a low-cost and stable CoMoP@C electrocatalyst superior to Pt/C. *Energy Environ. Sci.* **2017**, *10*, 788-798.

(31) Li, X. H.; Kurasch, S.; Kaiser, U.; Antonietti, M. Synthesis of monolayer-patched graphene from glucose. *Angew. Chem. Int. Ed.* **2012**, *51*, 9689-9692.

(32) Li, W.; Liu, Y.; Wu, M.; Feng, X.; Sat, R.; Shang, Y.; Yong, X.; Feng, T.; Wu, K.; Liu, Z. Carbon-quantum-dots-loaded ruthenium nanoparticles as an efficient electrocatalyst for hydrogen production in alkaline media. *Adv. Mater.* **2018**, *30*, 1800676.

(33) Morales-Guio, C. G.; Stern, L. A.; Hu, X. Nanostructured hydrotreating catalysts for electrochemical hydrogen evolution. *Chem. Soc. Rev.* **2014**, *43*, 6555-6569.

(34) Wang, J.; Xu, F.; Jin, H.; Chen, Y.; Wang, Y. Non-noble metal-based carbon composites in hydrogen evolution reaction: fundamentals to applications. *Adv. Mater.* **2017**, *29*, 1605838.

(35) Cui, X.; Ren, P.; Deng, D.; Deng, J.; Bao, X. Single layer graphene encapsulating non-precious

metals as high-performance electrocatalysts for water oxidation. *Energy Environ. Sci.* **2016**, *9*, 123-129.

(36) Deng, J.; Ren, P. J.; Deng, D. H.; Bao, X. H. Enhanced electron penetration through an ultrathin graphene layer for highly efficient catalysis of the hydrogen evolution reaction. *Angew Chem. Int. Ed.* Engl. **2015**, *54*, 2100-2104.

(37) Tran, D. T.; Kshetri, T.; Nguyen, D. C.; Gautam, J.; Hoa, V. H.; Le, H. T.; Kim, N. H.; Lee, J. H. Emerging core-shell nanostructured catalysts of transition metal encapsulated by two-dimensional carbon materials for electrochemical applications. *Nano Today* **2018**, *22*, 100-131.

TOC: